Fabrication and Characterization of Sericin-PVA Composite Films from *Gonometa postica*, *Gonometa rufobrunnea*, and *Argema mimosae*: Potentially Applicable in Biomaterials

Kanono Comet Manesa, Temesgen Girma Kebede,* Simiso Dube,* and Mathew Muzi Nindi

Read Online

ACCESS | Metrics & More | Article Recommendations | SI Supporting Information

ABSTRACT: This study deals with the fabrication and characterization of sericin-poly(vinyl alcohol) (PVA) composite films from three southern African silkworm cocoons. The sericin-PVA films were achieved by chemically cross-linking poly(vinyl alcohol) (PVA) with pure silk sericin protein using glutaraldehyde (GA) as a cross-linking agent. Fourier transform infrared (FTIR) results confirmed the overall cross-linking of pure silk sericin into PVA-GA networks to form cross-linked sericin-PVA films. This incident was shown by the incorporation of distinct major amide I (ν = 1640−1650 cm^{-1}), amide II (ν = 1538−1540 cm^{-1}), and amide III (ν = 1238−1244 cm^{-1}) peaks. X-ray diffraction (XRD) showed sericin-PVA films to have two features, one representing amorphous and crystalline regions of silk sericin and the other representing sharp high-intensity PVA peaks at around 2θ = 20.2°, demonstrating a high crystallinity in the

films as a result of the hydroxyl groups in its side chain. The swelling capacity of the three sericin-PVA films was influenced by the glutaraldehyde content used during the cross-linking process and pH of the aqueous medium into which the films were immersed after a period of time. The water contact angles of the sericin-PVA films were low, at 56.6 ± 0.56 and 60.2 ± 0.86, indicating further their hydrophilic nature. The scanning electron microscopy (SEM) images of the sericin-PVA films showed a rough texture with a granular network pattern on their surface. From the preliminary results, it was observed that the cytotoxicity of three sericin strains (*Gonometa rufobrunnea*, *Argema mimosae*, and *Gonometa postica*) had a cell viability percentage of 103, 90, and 80% respectively, demonstrating their biocompatibility in providing a favorable natural microenvironment for cell culture. The characterization results of the three silk sericin-PVA films demonstrated their potential for application in biomedical and biomaterial fields.
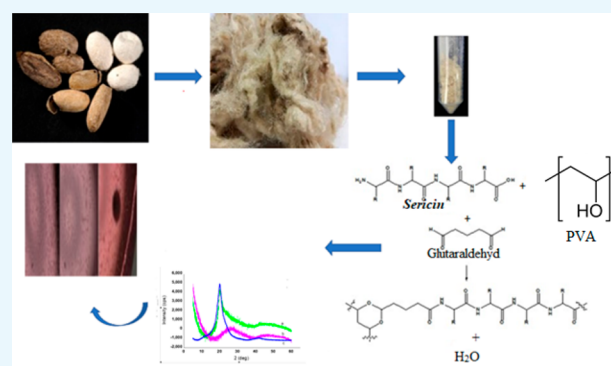
1. INTRODUCTION

The use of natural and synthetic polymer-based biomaterials for medical application has increased tremendously due to high demands from the medical industry to treat millions of patients yearly using different implantable devices and skin substitutes.[1] Based on these demands, manufacturers are being pressurized to explore alternative biomedical materials. This has created a shift of interest toward the use of natural polymer materials, which are biodegradable, biocompatible, environmentally friendly, and economical. The natural polymeric materials provide an essential advantage of flexibility in chemistry, offering a great diversity of chemical, physical, and mechanical properties.[2] These polymers are commonly known as biopolymers and are preferred due to their ability to support cell adhesion, migration, proliferation, and differentiation of cells from the surrounding environment. The structure and chemical composition of biopolymers are similar to those of macromolecules of the native extracellular environment. In addition, the biopolymers also induce extracellular matrix formation, which stimulates tissue repair, making them suitable

for tissue engineering applications.[3] Several biopolymers such as carbohydrates and proteins have been used in different medical applications. Among the protein biopolymers, chitosan, collagen, keratin, fibroin, and gelatin are the most utilized for biomaterial engineering.[4]

Silk sericin is a natural hydrophilic macromolecular protein, which is a byproduct of the degumming process during silk production. During this process, a large amount of sericin protein is usually discarded as waste.[5] Silk sericin protein is mainly constituted of 18 amino acids containing hydroxyl, carbonyl, and amino groups in their side chains. These functional groups enable silk sericin to readily cross-link, blend, and copolymerize with other polymers to produce improved

biomaterials with enhanced properties.[6−10] Silk sericin is postulated to possess unique properties such as antioxidant, antibacterial, and UV-B resistant; it regulates moisture and inhibits the activity of tyrosine kinase.[11,12] It is also capable of promoting wound healing by increasing collagen synthesis through activation of the fibroblast.[13,14] The films from sericin can regulate exudates (water, proteins, and electrolytes) of wounds, providing a moist environment for re-epithelialization and remodeling of connective tissues.[15] Sericin films also have a slow degradation, heightened fibroblast cell attachment, and cell viability, with efficient and effective skin repair application.[16]

Even though silk sericin holds several unique properties that have fascinated researchers from various biomaterial fields, its main challenge is that it cannot form a film on its own. This is because it is usually degraded during the harsh degumming process and results in an amorphous structure with a low molecular weight. Consequently, it cannot be cross-linked on its own to form a polymeric film. For this reason, silk sericin is subjected to a variety of modifications by widely blending or cross-linking with many other biopolymers or synthetic polymers to produce films that give improved properties.[17,18]

The focus of the study was to fabricate and characterize sericin-poly(vinyl alcohol) (PVA) films derived from native Southern Africa silkworm cocoons with the aim of exploring their cytocompatibility when used as a biomaterial. To the best of our knowledge, no study has been reported on the utilization of the three native sericin extracts for fabrication of films or any other forms such as hydrogels, fibers, and scaffolds. The findings of this study will contribute toward additional knowledge about the biological properties and possible biomaterial applications of native Southern African sericin extracts, namely *Gonometa postica*, *Gonometa rufobrunnea* (Lepidoptera: Lasiocampidae), and *Argema mimosae* (Lepidoptera: Saturniidae).

2. MATERIALS AND METHODS

2.1. Materials. All 20 L-amino acids standards, dabsyl-Cl, glacial acetic acid, ethanol, acetonitrile, 32% hydrochloric acid, acetone, glutaraldehyde (GA), glycerol, poly(vinyl alcohol), and dimethyl sulfoxide (DMSO) were all purchased from Sigma-Aldrich (Steinheim, Germany). Sodium carbonate, sodium hydrogen carbonate, sodium acetate, and sodium hydroxide pellets were all purchased from Merck (Darmstadt, Germany). All chemicals and reagents were of analytical grade (95−99% purity). Water was generated from a Milli-Q system with a resistivity of 18.2 MΩ cm^{-1} (Millipore, Billerica, MA) and used for preparation of solutions.

2.2. Silk Sericin Samples. Silk sericin was obtained from three wild Southern African silkworm cocoons. *G. postica* cocoons were harvested from Eastern Cape in South Africa. *G. rufobrunnea* cocoons were gathered at Shashe in Botswana. *Argema mimosae* cocoons were collected from the Manzini district in eSwatini (formerly Swaziland). The silk cocoons were degummed using a BioLAB vertical autoclave (BAVT-101, Canada) for 1 h 45 min at a temperature of 120 °C. After autoclaving, the degummed cocoons were filtered to separate sericin from fibroin filaments. The filtered sericin was preconcentrated and then lyophilized into sericin powder with a KK freeze dryer (FD-10, China).

2.3. Preparation of Sericin-PVA Films. Sericin-PVA films were prepared by dissolving about 400 mg of PVA, into 7 mL of ethanol (3% v/v) and glycerol (1% w/v) solution, which was heated prior in a microwave for 3.0 min. The mixture was stirred for 1 h at a temperature of 80 °C, to allow for complete dissolution of PVA. The solution was acidified with 1.0 mL of 0.05N HCl. This was followed by the addition of 1.0 mL diluted aqueous solutions of different percentages (0.3−3% v/v) of glutaraldehyde (GA) for cross-linking. The mixture was stirred for 5.0 min before 1.0 mL of (3% w/v) sericin was added. The solution was stirred for 2 h, and the temperature was increased to 90 °C to promote a homogeneous mixture. Cross-linked solutions were cast into glass Petri dishes and then allowed to cool overnight at room temperature before being dried in an oven at 65 °C for 24 h. The dried films were moisturized with 70% ethanol and then allowed to dry for 4 h before being peeled off. The films were thoroughly washed with distilled water and dried at 60 °C for 12 h before being stored in a conditioned desiccator until characterization.

2.4. Characterization of Sericin-PVA Films.
2.4.1. Amino Acid Analysis. To determine the amino acid composition, 10 mg of silk sericin was hydrolyzed in 2 mL of 6M HCl at 110 °C for 24 h. About 50 μL of the hydrolyzed sericin was transferred into microcentrifuge tubes for derivatization with Dabsyl-Cl. The derivatized silk sericin hydrolysates were dried and redissolved in 4 mL of ethanol. Amino acid analysis was achieved with an Agilent 1200 HPLC−DAD system (Waldbronn, Germany). The instrument was fitted with Agilent Chemstation data software. An Agilent Zorbax Eclipse XDR C18 (4.5 × 150 mm^2, 5 μM) column was used for the separation of 18 amino acids, of which 9 were polar.

2.4.2. Fourier Transform Infrared analysis of Sericin-PVA films. The secondary structural transition of sericin-PVA films was determined using an attenuated total reflection fourier transform infrared (ATR-FTIR) spectrophotometer (Brucker Vertex 70 manufactured in Ettlingen, Germany), which incorporated a single-reflection diamond ATR attachment. All spectra were obtained at room temperature within a wavenumber range of 600−4000 cm^{-1} with acquisition of 32 scans at 4 cm^{-1} resolution. FTIR was also used for the confirmation of the cross-linking reaction between the three silk sericin extracts and PVA at two different percentages of glutaraldehyde (1 and 3%).

2.4.3. X-Ray Diffraction (XRD). The crystallinity of the sericin-PVA films was analyzed with a Rigaku SmartLab 9 kW, high-resolution X-ray diffraction system using Cu Kα radiation for the determination of diffraction intensity curves. These were obtained at λ = 1.5 Å for 2θ from 10 to 60° at a scanning rate of 0.0015° s^{-1}. Voltage and current of the X-ray source were 45 kV and 200 mA, respectively.

2.4.4. Percentage Swelling of Sericin-PVA Films. The percentage swelling test of the films was determined as reported by Mandal et al. with slight modifications.[17] Conditioned films were placed in an oven at 40 °C over a period of 12 h and weighed thereafter using a ML series Mettle Toledo balance (Greifensee, Switzerland). The dried films were immersed in 50 mL of distilled H$_2$O, 0.1 N HCl, and 0.1 N NaOH for 4 h. After 4 h, the films were taken out, and the excess solution was blotted with a filter paper. The effect of time on % swelling was studied at different time intervals from 0.5 to 4 h. The experiments were done in quintet to determine the standard deviation (SD) of each measurement. The percentage swelling of the sericin-PVA films at equilibrium was calculated using the equation given below

$$\% \text{ swelling} = \frac{W_{sw} - W_{dw}}{W_{dw}}$$

where W_{sw} is the weight of the swollen film and W_{dw} is the weight of the dried film.

2.4.5. Water Contact Angle of Sericin-PVA Films. The wettability of the sericin-PVA films was evaluated using a sessile drop technique. Cross-linked sericin-PVA films were prepared on glass slides, and then, the water contact angles were measured by dropping 5 μL of ultrapure water onto the sericin-PVA films' surfaces. The contact angle measurements and images were automatically taken using a contact angle analyzer at 25 °C. The contact angles were observed at an interval of 5 s, and the average of at least six measurements was recorded.

2.4.6. Scanning Electron Microscopy (SEM) Analysis of Sericin-PVA Films. The sericin-PVA films were cut into pieces and equilibrated in 53% relative humidity prior to analysis. All the films were sputter-coated with gold and then examined using a JEOL scanning electron microscope (JSM-IT300HR, Japan) at an accelerating beam voltage of 20 kV.

2.5. Cell Culture. HEK293 cells that were specifically derived from human embryonic kidney cells, from an aborted female fetus, which were grown in a tissue culture[19] of an unknown passage, were cultured and maintained in Dulbecco's modified Eagle medium (DMEM), fetal bovine serum (FBS), and 1% penicillin/streptomycin (Pen/Strep). The cells were serially passaged until they showed ∼70% confluency and were then seeded in a 96-well for 24 h to ensure attachment.

2.5.1. Cell Viability Assay. The reduction of 3-[4,5-dimethylhiazol-2-yl]-2,5-diphenyl tetrazolium bromide (MTT) during cell proliferation includes the conversion of MTT into formazan crystals by living cells by mitochondrial succinate dehydrogenase enzyme activity; this in turn controls the measurement of viable cells and determination of their mortality. The MTT cytotoxicity assay was conducted in accordance with the method described by More and Makola.[20] In this study, the cytotoxicity effects of various sericin-PVA film solutions were determined on human embryonic kidney (HEK293) cells. The sericin-PVA film solutions were serially diluted to obtain concentrations ranging from 1.56 to 100 μg/mL. The experiment was conducted on a microtiter plate by seeding aliquots of 100 μL of the cell suspension at 1×10^5 cells/well; to enhance cell attachment, the cells were incubated in a 5% CO_2 chamber at 37 °C for 24 h. After the 24 h period, the medium was aspirated and replaced with 100 μL of fresh media and sericin-PVA solutions in triplicate. The plates were then washed with pure dimethyl sulphoxide (DMSO) to remove the remaining medium and returned to the incubation chamber for a further 48 h.

In the experiment, untreated cells and doxorubicin chloride were included as negative and positive controls, respectively. After incubation, 50 μL of 5 mg/mL MTT solution (Sigma-Aldrich, Germany) was added to each well and returned to the chamber for 3 h. Subsequently, 100 μL of DMSO was added to all the wells as a solubilizing agent to dissolve any formed formazan dark-blue crystals, and the microtiter plates were then incubated for a further hour. The plates were then read at an absorbance of 570 nm using a UV-spectrophotometer (Varioskan Flash, Thermofischer Scientific) and a reference wavelength of 630 nm. The percentage of viable HEK293 cells was then plotted against the respective test concentrations.

The total cell viability of the cells was calculated using the cell viability formula

$$\text{cell viability (\%)} = [AT/AC] \times 100$$

where AT is the absorbance of sericin film/positive control-treated cells and AC is the absorbance of untreated cells.

2.6. Statistical Analysis. Experimental measurements were conducted in triplicate, and the data were expressed as the mean ± standard deviation (SD) for $n = 4$. Analysis of data was performed using variance at a 95% confidence level, standard error, fitted regression equation, and coefficient of correlation (ANOVA, Microsoft Excel Office 2010). Statistical differences were considered as statistically significant when $p < 0.05$.

3. RESULTS AND DISCUSSION

3.1. Amino Acid Composition of Three Wild-Silk Sericin Proteins. The hydrophilicity of the silk sericin protein is usually determined by the type and amount of polar amino acids. The polar amino acid composition of the sericin protein derived from *G. postica*, *G. rufobrunnea*, and *A. mimosae* silkworm cocoons is presented in Table 1. The results indicate

Table 1. Percentage Compositions (mol % ± SD) of Polar Amino Acids from the Three Silk Sericin Species

|	sericin protein extracts		
amino acid	*G. postica* (GP)	*G. rufobrunnea* (GR)	*A. mimosae* (Sat)
serine	29.7 ± 0.17	21.39 ± 0.10	20.78 ± 0.15
histidine	1.36 ± 0.04	1.07 ± 0.11	2.0 ± 0.2
aspartic acid[a]	16.74 ± 0.20	12.32 ± 0.10	14.09 ± 0.16
glutamic acid[b]	9.80 ± 0.15	8.95 ± 0.05	7.92 ± 0.10
arginine	4.92 ± 0.07	3.62 ± 0.02	4.41 ± 0.02
cysteine	0.33 ± 0.01	0.07 ± 0.01	0.12 ± 0.01
threonine	3.38 ± 0.06	2.29 ± 0.02	3.20 ± 0.03
lysine	1.68 ± 0.03	1.50 ± 0.01	1.49 ± 0.02
tyrosine	3.80 ± 0.06	2.81 ± 0.02	3.47 ± 0.04

[a]Aspartic acid is the combination of aspartic acid and asparagine.
[b]Glutamic acid is the combination of glutamic acid and glutamine.

that *G. postica* sericin has the highest content of hydrophilic amino acids, followed by *A. mimosae* and *G. rufobrunnea* in that order. *G. postica* sericin consisted of 29.7, 16.74, and 9.80% of serine, aspartic acid, and glutamic acid, respectively. For both *G. rufobrunae* and *A. mimosae* sericin, the above-mentioned amino acids are in higher compositions, but in lower contents compared what is found in *G. postica* sericin proteins. Polar amino acid compositions were found to play an essential role in sericin film intrinsic properties. The amino acid compositions are found to influence the stability and solubility of the sericin films due to the presence of intermolecular disulfide linkages and the polar amino acid moieties. On the other hand, solubility is also influenced by the availability of the polar functional groups. Barone and co-workers[21] also reported on the influence of these polar amino acids on the characteristics of feather keratin.

3.2. Structural Studies of Sericin-PVA Films. *3.2.1. FTIR Characteristics of Sericin-PVA Films.* Figures 1−3 represent three secondary structural spectra of sericin-PVA composite films (*GR-SPF, GP-SPF,* and *Sat-SPF*) characterized by FTIR. Pure sericin spectra were also included (Figures 1a, 2a, and 3a) as references, to identify major peaks and highlight changes in
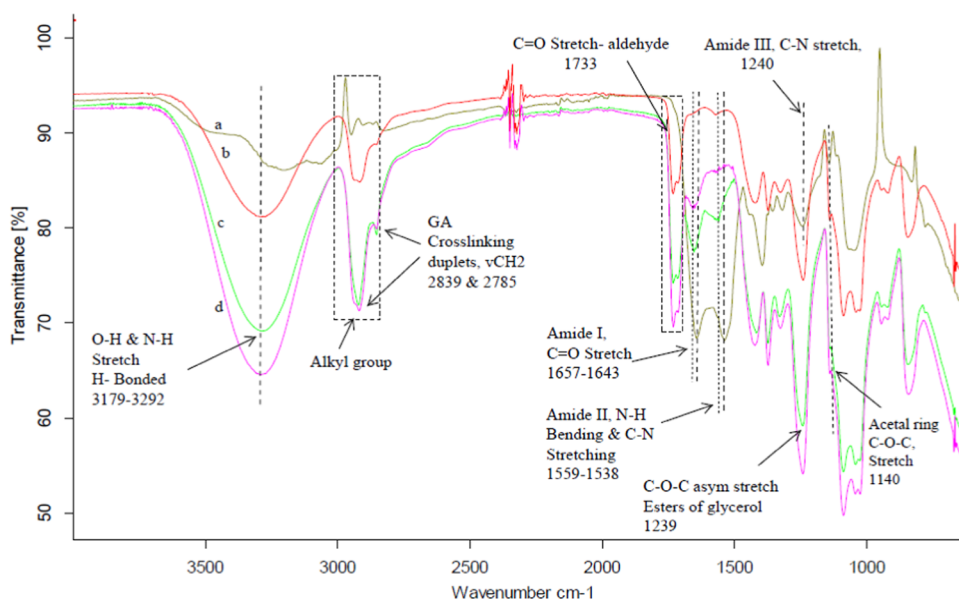
Figure 1. *G. postica* sericin-PVA films, (a) pure sericin, (b) PVA, (c) 3% glutaraldehyde cross-linked sericin filmm, and (d) 1% glutaraldehyde cross-linked film.
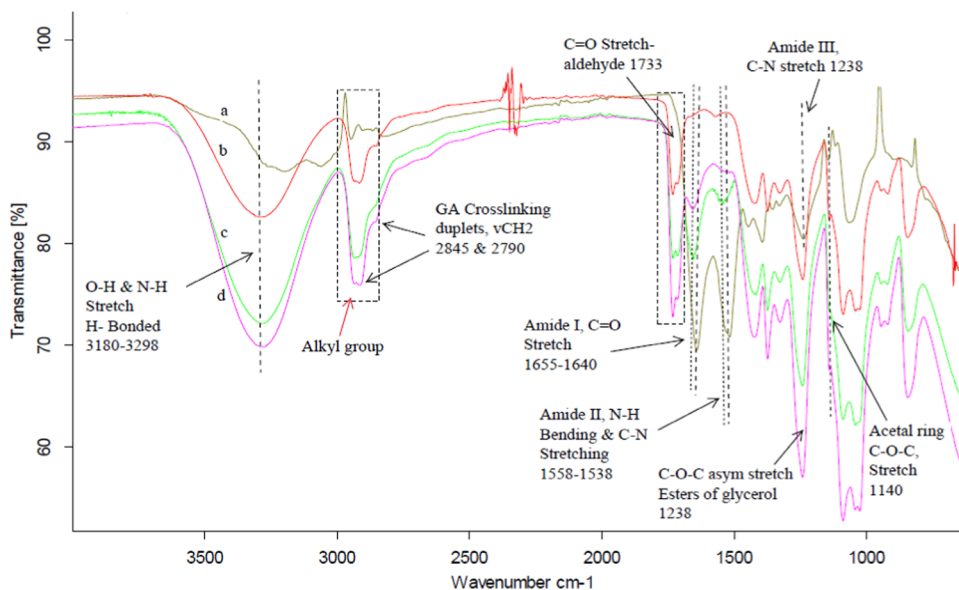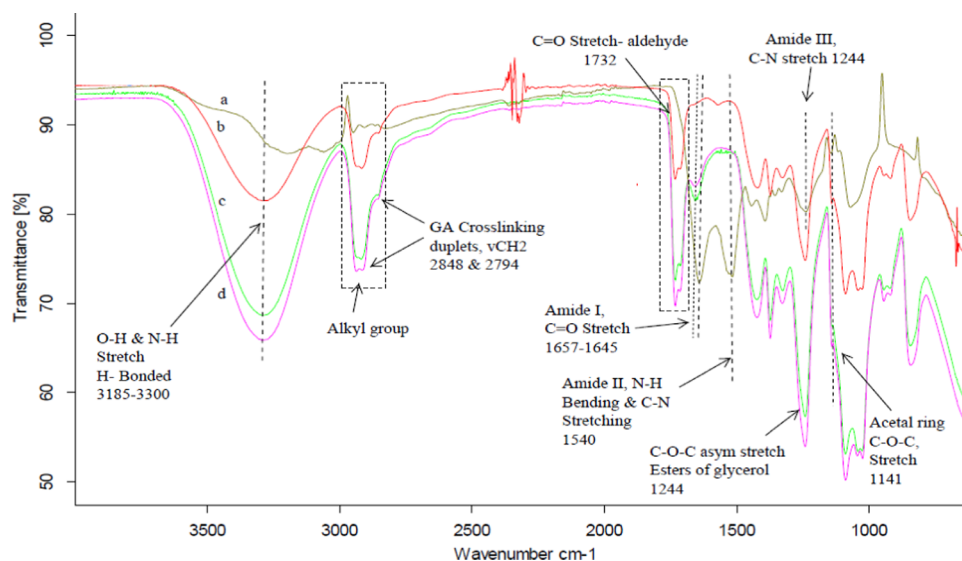

Figure 2. *G. rufobrunnea* sericin-PVA films, (a) pure sericin, (b) PVA, (c) 3% glutaraldehyde cross-linked sericin film, and (d) 1% glutaraldehyde cross-linked sericin film.

the secondary structural transition before and after cross-linking. The three spectra (Figures 1−3) illustrate all major peaks associated with the PVA-GA (hydroxyl and acetate groups) network and those that demonstrate silk sericin incorporation. The three sericin-PVA films showed weak to medium, broad hydrogen-bonded bands that result from the overlap of free and bound OH and NH stretching vibrations at 3179−3300 cm^{-1}. The hydrogen bond is a result of the intermolecular and intramolecular interaction between the OH groups of PVA and CO and NH group of the incorporated silk sericin protein.

Two important vibrational bands at 2884 and 2839 cm^{-1} of C−H stretching are associated with aldehydes, duplet absorption peaks attributed to the alkyl chain.[22] When PVA is cross-linking with GA, the intensity of the OH stretching vibration peaks between 3275 and 3300 cm^{-1} was notably

reduced as compared to that of pure PVA, which is an indication of the formation of acetal bridges. Also, the presence of strong aldehyde peaks at 1732−1733 cm^{-1} is a result of C= O stretching, indicating the incomplete reaction of the aldehyde group (C=O) with OH groups of the PVA chain or possibly the contribution of the remaining acetate groups of the PVA structure.[23] An important absorption peak at 1141 cm^{-1} indicates the C−O stretching, which has been used to assess the pure PVA semicrystalline structure. During cross-linking, this peak (C−O stretching) is replaced by a broader absorption peak attributed to ether (C−O) and acetal ring (C−O−C) peaks produced during the cross-linking reaction of PVA with GA.[24,25] This observed peak confirms that GA acted as a cross-linking agent among PVA polymeric chains.

In addition, major amide absorption peaks associated with three secondary structural transition spectra of sericin-PVA
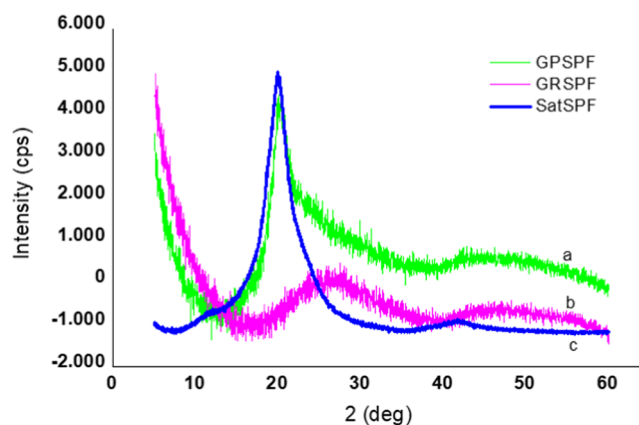
Figure 3. *A. mimosae* sericin-PVA films, (a) pure sericin, (b) PVA, (c) 3% glutaraldehyde cross-linked sericin film, and (d) 1% glutaraldehyde crosslinked film.

films were observed. Peaks associated with amide I absorption bands are at 1643, 1640, and 1650 cm^{-1} for *GP-SPF*, *GR-SPF*, and *Sat-SPF*, respectively, associated with the C=O stretching vibration.

Absorption bands for amide II at 1538 cm^{-1} (*GP-SPF* and *GR-SPF*) and 1540 cm^{-1} for *Sat-SPF* are a result of N−H bending and C−N stretching vibrations. Amide III bands at 1238 (*GP-SPF*), 1244 cm^{-1} (*Sat-SPF*), and 1239 cm^{-1} (*GR-SPF*) were mainly from C−N stretching coupled to N−H bending vibration. Amide III is regarded as a signature peak for silk sericin protein and is usually a weak peak in FTIR. Silk sericin incorporation within the PVA/GA network confirms the success of the cross-linking process that occurred between OH groups of PVA and the CO and NH groups of the silk sericin. This is supported by the shifts of the amide I absorption peaks from the pure sericin from their original absorption peaks at 1640, 1643, and 1645 cm^{-1} to 1655, 1657, and 1657 cm^{-1}, respectively. The average change was found to be around 14 cm^{-1}, moving to a higher wavenumber. Amide I absorption peaks for pure sericin are assigned to the random coil. It was noted that after sericin incorporation within the PVA/GA network, there was evidence of a shift toward a α-helix. For pure sericin amide II, absorption peaks occur at 1538 cm^{-1} for both *Gonometa* sericin extracts and at 1540 cm^{-1} for *A. mimosae* sericin. These peaks were all attributed to the α-helix structure. After incorporation of sericin within the PVA/GA network, amide I and II showed a shift of around 20 cm^{-1}. In the case of *Sat-SPF*, amide I also showed a shift of ∼20 cm^{-1}, while there was no evidence of an amide II shift. The presence of the strong intensity of glycerol at 1238−1244 cm^{-1} (related to C−O−C asym stretching) decreases the intensity of amide I, II, and III peaks. As a result, this shows that glycerol increases the development of the α helix structure.[26]

3.2.2. X-Ray Diffraction Analysis. During the cross-linking process, glutaraldehyde binds the hydroxyl (−OH) groups of PVA with sericin polar (−OH and NH) groups. As a result, the number of hydroxyl groups for both compounds is depleted due to the complete cross-linking reaction, causing a decrease in the crystallinity of the film. Figure 4 shows the X-ray diffractograms of the three sericin-PVA films (*GR-SPF, GP-*
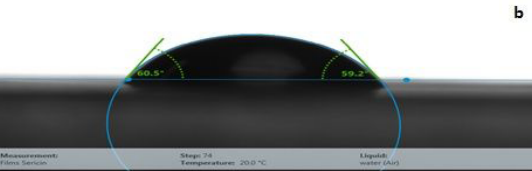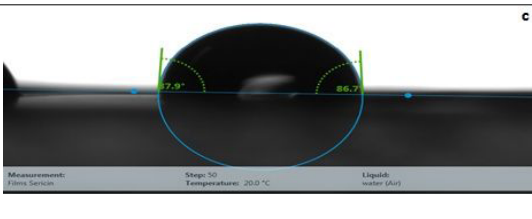

Figure 4. Illustration X-ray diffractograms of (a) *G. postica* sericin-PVA film, (b) *G. rufobrunnea* sericin-PVA film, and (c) *A. mimosae* sericin-PVA film.

SPF, and *Sat-SPF*). The cross-linking in the films (*GP-SPF* and *Sat-SPF*) is confirmed by the amorphous feature characteristic of sericin and the crystalline regions associated with PVA. The peaks at around $2\theta = 20.2°$ demonstrate high crystallinity in the films as a result of the hydroxyl groups. The crystallinity observed in the case of *GP-SPF* and *Sat-SPF* films could be associated with the high amount of polar amino acids. It is assumed that during cross-linking, not all polar groups from PVA and sericin undergo the cross-linking reaction, which means that there is no complete depletion of their hydroxyl groups. The peaks for *GP-SPF* were at around $2\theta = 14.2$ and 24°, while *Sat-SPF* peaks (Figure 4c) were found at $2\theta = 14.8$ and 24.6°. In addition, typical crystalline PVA shoulder peaks were observed for both *GP-SPF* and *Sat-SPF* films at around $2\theta = 46.6$ and 42°, respectively.

In contrast with the sericin-PVA films mentioned above, the results of the *GR-SPF* film (Figure 4b) show a single broad flat peak of low intensity around $2\theta = 26.2°$. This peak is a result of an amalgamation between PVA and sericin, which results in the loss of the characteristic peak at $2\theta = 19.6°$ for the former and at around $2\theta = 19.2$ and 23.2° for the latter. The characteristic PVA shoulder peak was observed at around $2\theta =$

Table 2. Water Contact Angles Measured on Various Sericin-PVA Films[a]

Films	Water contact angle (X°)	Photographs of contact angle
GP-SPF	56.6 ± 0.56	
Sat-SPF	60.2 ± 0.86	
GR-SPF	86.7 ± 0.60	

[a]Tests were measured in five different sides each in triplicate.

47.2°, confirming the cross-linking. Also, the peak intensity of the *GR-SPF* film was lower than that of the peaks observed for both *GP-SPF* and *Sat-SPF* films, suggesting that its overall crystallinity was slightly lower than that of the other two films due to its low number of polar groups.

3.3. Sericin-PVA Films' Degree of Swelling. Swelling is an effective indirect method for determining the real degree of cross-linking for polymeric networks. As illustrated in Supporting Data 1, the swelling response of the three sericin-PVA films (*GR-SPF, GP-SPF,* and *Sat-SPF*) cross-linked with various concentrations of glutaraldehyde (GA), after immersing in distilled H$_2$O, 0.1 M NaOH, and 0.1 M HCl for 4 h. The results presented also show that an increase in the glutaraldehyde concentration resulted in a decrease in the swelling capacity of the films. The observed decrease in swelling is a result of a decline in the number of free hydroxyl groups that are available for the water interaction. At 0.3% concentration of glutaraldehyde, both *G. postica* and *A. mimosae sericin-PVA* films were entirely dissolved in the three aqueous media due to their high number of amino acids with polar groups, which provide the two films with additional hydroxyl groups even after cross-linking. In contrast, for *GR-SPF*, swelling was observed at 0.3% glutaraldehyde without the film dissolving in the three aqueous media. All films cross-linked with 3.0% glutaraldehyde attained equilibrium faster and had a slightly lower degree of swelling compared with those that were cross-linked with a lower concentration (0.3−0.8%). At a concentration greater than 3.0% glutaraldehyde, a transparent glass-like hydrogel was formed instead of the films. The decrease in the degree of swelling is an indicator that there is a compact cross-linking structure. Such a structure with a high cross-linking density results in smaller spaces within the molecules; therefore, less water can be absorbed.[27]

The degree of swelling was in the order of *GP-SPF > Sat-SPF > GR-SPF*, which is in line with the extent of cross-linking density and abundance of polar amino acids.

3.3.1. Effect of Time on the Degree of Swelling. The effect of time on the degree of swelling of the three sericin-PVA films after immersing in three aqueous media (Dist. H$_2$O; 0.1 M NaOH; and 0.1 M HCl) is presented in Supporting Data 2. Films cross-linked with a concentration of 3% glutaraldehyde were selected as ideal for this study due to their sorption properties. These films showed a stable swelling capacity compared to that of other films that were cross-linked with a smaller amount of glutaraldehyde.

The degree of swelling for the *GP-SPF* film showed an increasing swelling pattern even after the 5 h time limit that was set up for this study. This is attributed to an available space and a high number of OH groups that were still available to interact with water after cross-linking. In the case of both *GR-SPF* and *Sat-SPF* films, the degree of swelling was also faster; however, at around 3 h of immersion, the swelling rate becomes slower. This saturation is attributed to a depletion of the OH groups, available for the water interaction, causing a further restriction of space in a film network. Therefore, as time progresses, this leads to a lesser absorption of water due to the water concentration gradient that presents partial back pressure within the film.

3.4. Contact Angle Measurement of Sericin-PVA Films. The water contact angle measurement using a sessile drop method was utilized to evaluate the wettability of the three sericin-PVA films. The results of the water contact angle for the three films are shown in Table 2. Both *GP-SPF* and *Sat-SPF* showed low contact angles of 56.6 ± 0.56 and 60.2 ± 0.86, respectively, compared to the contact angle of 86.7 ± 0.60 obtained for *GR-SPF*. The wettability was in the order of GP-

SPF > *Sat-SPF* > *GR-SPF*. The highest contact angle was evidence of hydrophobicity. The residual hydroxyl groups in the cross-linked structure interacted with water molecules in the water drop. Hence, the water drop was attracted and adhered more to the surface of the films, resulting in low contact angle values, which shows the hydrophilic character.[28]

3.5. Microscopic Structure of Sericin-PVA films. The surface morphology of the three sericin-PVA films is shown in Figure 5a−c. Both *GP-SPF* and *Sat-SPF* films showed a homogeneous smooth surface, compared to the *GR-SPF* film, which had a rough surface with small-sized spherical globular
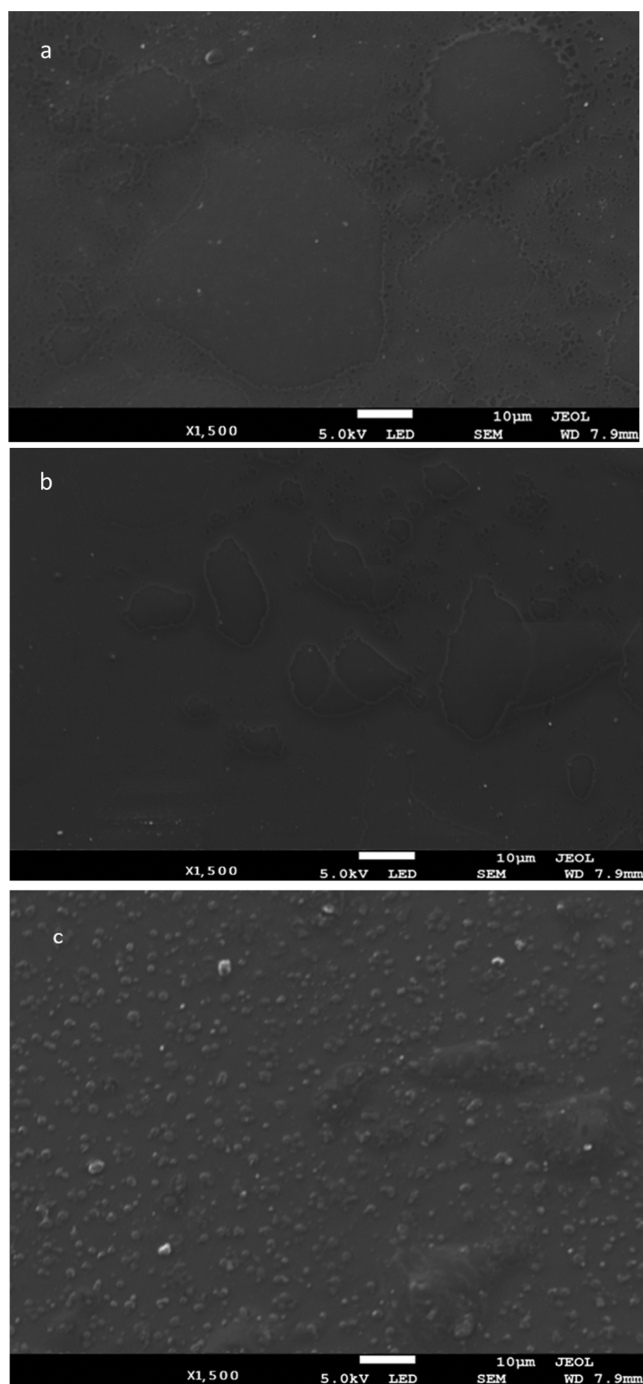
Figure 5. Scanning electron microscopy photos of the three sericin-PVA films: (a) GP-SPF, (b) Sat-SPF, and (c) GR-SPF.

particles (nanoscale) distributed throughout the film surface. These many spherical granules are ascribed to excess GA that was left during cross-linking of sericin polar side groups and the -OH of PVA, resulting in a heterogeneous structure. The smooth surfaces found in both *GP-SPF* and *Sat-SPF* films indicate the contribution of GA and glycerol in enhancing the miscibility of PVA and silk sericin. Both GA and glycerol were found to reduce the phase separation of the films. *GP-SPF* and *Sat-SPF* films at higher magnification showed embedded sericin particles within the films' surface. These prominent features found on the surface of the films provide extra surface area, that present adhesion potential for future biomedical applications.

3.6. Preliminary Test on the Biocompatibility of Sericin-PVA Films. *3.6.1. Cell Viability on Sericin-PVA Films.* The effects of cytotoxicity on HEK293 cells by sericin-PVA solutions at doses of 1.5625; 3.125, 6.25; 12.5; 25; 50; and 100 μg/mL were investigated at an exposure time of 48 h. Figure 6 shows how the concentrations used in this study had a significant impact on cell viability over the entire concentration range of sericin solutions. This behavior confirms the suitability of the sericin solution as a possible growth factor for HEK293 cells. In comparing the cytotoxicity effects of the three strains of sericin solutions, it was discovered that the lowest concentration of 1.5625 μg/mL for the three strains, namely *G. rufobrunnea*, *A. mimosae*, and *G. postica*, had a cell viability percentage of 103, 90, and 80% respectively. When comparing the effect of cell viability at the highest concentrations of sericin solution, *G. rufobrunnea* and *A. mimosae* had viable cells of 74 and 72%, respectively. However, in the case of *G. postica* sericin, the HEK293 cells were at around 62% viability. Figure 7 shows a moderate dose-dependent response of HEK293 cells toward the three sericin strains. The HEK293 cell response demonstrates a weak biphasic sericin solution effect, where a low concentration would provide a high HEK293 cell viability and a high concentration would inhibit HEK293 cell viability. However, in this study, even at a high concentration, the viability of the HEK293 cells was still above 60% for all the sericin strains, which means that the three sericin strains produce low mortality of HEK293 cells across the entire concentration range. These findings confirm how the concentration of the sericin solution in the casted sericin-PVA films plays a significant growth role in cell viability.

4. CONCLUSIONS

The results of this study demonstrate how the three fabricated sericin-PVA films presented comparable features as the other composite films from the commonly used biopolymers (chitosan, fibroin, collagen, gelatin, alginates, etc.). This was observed when the three sericin-PVA films were characterized for chemical, physical, and biological properties. The three sericin extracts were found to contain high polar amino acids that are considered important for cross-linking and water absorption. Cross-linking of sericin and PVA provided stable, insoluble sericin-PVA films that only swell when immersed in three different aqueous solutions. The swelling capacity of sericin-PVA films provided a satisfactory proof of a successful glutaraldehyde cross-linking process. The findings of this study suggest that the three fabricated sericin-PVA films are biocompatible and may offer potential benefits to being used for various biomedical applications. However, an extensive investigation should be conducted to understand the cell
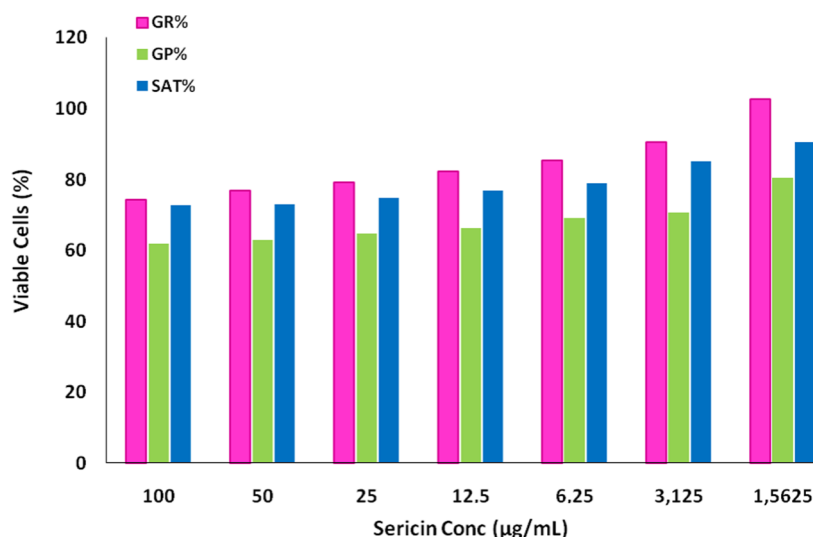
Figure 6. Percentage of viable HEK293 cells in the presence of (GR) *G. rufobrunnea*; (GP) *G. postica*; and (SAT) *A. mimosae* film solutions.
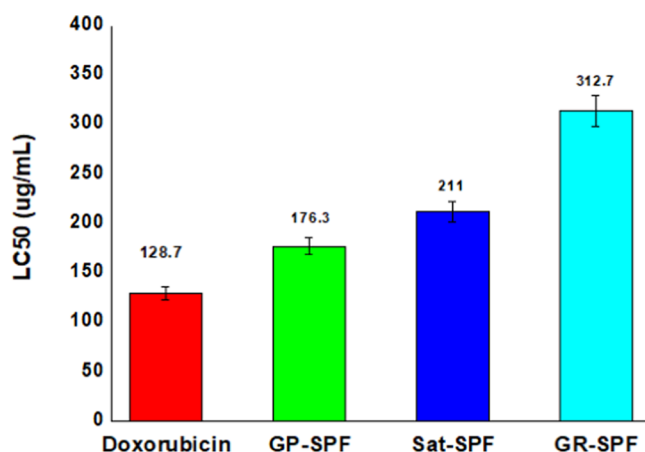

Figure 7. LC$_{50}$ of *G. rufobrunnea*, *A. mimosa*, and *G. postica* sericin solutions (mean + standard error) exposed to HEK293 cells for 48 h.

adhesion, proliferation, and viability of various cell lines on the fabricated sericin-PVA films.

■ ASSOCIATED CONTENT

ⓢ Supporting Information

The Supporting Information is available free of charge at https://pubs.acs.org/doi/10.1021/acsomega.2c00897.

> Percentage swelling capacity of *A. mimosae* sericin/PVA films cross-linked with different concentrations of glutaraldehyde (GA), percentage of viable HEK293 cells in the presence of *G. rufobrunnea*; *G. postica*; and *A. mimosae* film solutions, and percentage swelling of GR-SPF, GP-SPF, and Sat-SPF (cross-linked with 3% GA) after being immersed over a time (PDF)

■ AUTHOR INFORMATION

Corresponding Authors

Temesgen Girma Kebede − *Department of Chemistry, University of South Africa, Roodepoort 1709, South Africa;* ⓞ orcid.org/0000-0001-7083-1772; Email: tgkkebede@gmail.com

Simiso Dube − *Department of Chemistry, University of South Africa, Roodepoort 1709, South Africa;* Email: dubes@unisa.ac.za

Authors

Kanono Comet Manesa − *Department of Chemistry, University of South Africa, Roodepoort 1709, South Africa*

Mathew Muzi Nindi − *Institute for Nanotechnology and Water Sustainability (iNanoWS), College of Science, Engineering and Technology, University of South Africa, Roodepoort 1709, South Africa*

Complete contact information is available at:
https://pubs.acs.org/10.1021/acsomega.2c00897

Notes

The authors declare no competing financial interest.

■ ACKNOWLEDGMENTS

■ REFERENCES

(1) Simchi, A.; Tamjid, E.; Pishbin, F.; Boccaccini, A. R. Recent progress in inorganic and composite coatings with bactericidal capability for orthopaedic applications. *Nanomed., Nanotechnol., Biol. Med.* **2011**, *7*, 22−39.

(2) Gulrajani, M. L. In *Sericin: A Biomolecule of Value*, Souveni 20th Congress of the International Sericultural Commission, Bangalore, India, 15−18 December, 2005; pp 21−29.

(3) Ulery, B. D.; Nair, L. S.; Laurencin, C. T. Biomedical applications of biodegradable polymers. *J. Polym. Sci., Part B: Polym. Phys.* **2011**, *49*, 832−864.

(4) He, C.; Zhuang, X.; Tang, Z.; Tian, H.; Chen, X. Stimuli-sensitive synthetic polypeptide-based materials for drug and gene delivery. *Adv. Healthcare Mater.* **2012**, *1*, 48−78.

(5) Levin, B.; Rajkhowa, R.; Redmond, S. L.; Atlas, M. D. Grafts in myringoplasti: Utilizing a silk fibroin scaffold as a novel device. *Expert Rev. Med. Devices* **2009**, *6*, 653−664.

(6) Wang, Z.; Zhang, Y.; Zhang, J.; Huang, L.; Liu, J.; Li, Y.; Zhang, G.; Kundu, S. C.; Wang, L. Exploring natural silk protein sericin for regenerative medicine: An injectable, photoluminescent, cell-adhesive 3D hydrogel. *Sci. Rep.* **2014**, *4*, No. 7064.

(7) Cho, K. Y.; Moon, J. Y.; Lee, Y. W.; Lee, K. G.; Yeo, J. H.; Kweon, H. Y.; Kim, K. H.; Cho, C. S. Preparation of self-assembled silk sericin nanoparticles. *Int. J. Biol. Macromol.* **2003**, *32*, 36−42.

(8) Zhang, Y.-Q. Applications of natural silk protein sericin in biomaterials. *Biotechnol. Adv.* **2002**, *20*, 91−100.

(9) Lim, K. S.; Kundu, J.; Reeves, A.; Poole-Warren, L. A.; Kundu, S. C.; Martens, P. J. The Influence of Silkworm Species on Cellular Interactions with Novel PVA/Silk Sericin Hydrogels. *Macromol. Biosci.* **2012**, *12*, 322−332.

(10) Kundu, B.; Kundu, S. C. Silk sericin/polyacrylamide in situ forming hydrogels for dermal reconstruction. *Biomaterials* **2012**, *33*, 7456−7467.

(11) Siqin, Z.; Yanaka, N.; Sasaki, M.; Watanabe, H.; Kato, N. Silk protein, sericin, suppresses DMBA-TPA-induced mouse skin tumorigenesis by reducing oxidative stress, inflammatory responses and endogenous tumor promoter TNF-a. *Oncol. Rep.* **2003**, *10*, 537−543.

(12) Takeuchi, A.; Ohtsuki, C.; Miyazaki, T.; Kamitakahara, M.; Ogata, S. I.; Yamazaki, M.; Furutani, Y.; Kinoshita, H.; Tanihara, M. Heterogeneous nucleation of hydroxyapatite on protein: Structural effect of silk sericin. *J. R. Soc. Interface* **2005**, *2*, 373−378.

(13) Sugihara, A.; Suglura, K.; Morita, H.; Ninagawa, T.; Tubouchi, K.; Tobe, R.; Mamoru Izumiya, J.; Horio, T.; Abraham, N. G.; Ikehara, S. Promotive Effects of a Silk Film on Epidermal Recovery from Full-Thickness Skin Wounds (44552). *Proc. Soc. Exp. Biol. Med.* **2000**, *225*, 58−64.

(14) Min, B.; Lee, G.; Hyun, S.; Sik, Y.; Seung, T.; Ho, W. Electrospinning of silk fibroin nanofibers and its effect on the adhesion and spreading of normal human keratinocytes and fibroblasts in vitro. *Biomaterials* **2004**, *25*, 1289−1297.

(15) Sapru, S.; Das, S.; Mandal, M.; Ghosh, A. K.; Kundu, S. C. Prospects of nonmulberry silk protein sericin-based nanofibrous matrices for wound healing − In vitro and in vivo investigations. *Acta Biomater.* **2018**, *78*, 137−150.

(16) Nayak, S.; Talukdar, S.; Kundu, S. C. Potential of 2D crosslinked sericin membranes with improved biostability for skin tissue engineering. *Cell Tissue Res.* **2012**, *347*, 783−794.

(17) Mandal, B. B.; Priya, A. S.; Kundu, S. C. Novel silk sericin/gelatin 3-D scaffolds and 2-D films: Fabrication and characterization for potential tissue engineering applications. *Acta Biomater.* **2009**, *5*, 3007−3020.

(18) Mandal, B. B.; Ghosh, B.; Kundu, S. C. Non-mulberry silk sericin/poly (vinyl alcohol) hydrogel matrices for potential biotechnological applications. *Int. J. Biol. Macromol.* **2011**, *49*, 125−133.

(19) Yuan, J.; Xu, W. W.; Jiang, S.; Yu, H.; Poon, H. F. The scattered twelve tribes of HEK293. *Biomed. Pharmacol. J.* **2018**, *11*, 621−623.

(20) More, G. K.; Makola, R. T. In-vitro analysis of free radical scavenging activities and suppression of LPS-induced ROS production in macrophage cells by Solanum sisymbriifolium extracts. *Sci. Rep.* **2020**, *10*, No. 6493.

(21) Barone, J. R.; Schmidt, W. F.; Gregoire, N. T. Extrusion of feather keratin. *J. Appl. Polym. Sci.* **2006**, *100*, 1432−1442.

(22) Mansur, H. S.; Oréfice, R. L.; Mansur, A. A. P. Characterization of poly(vinyl alcohol)/poly(ethylene glycol) hydrogels and PVA-derived hybrids by small-angle X-ray scattering and FTIR spectroscopy. *Polymer* **2004**, *45*, 7193−7202.

(23) Mansur, H. S.; Mansur, A. A. P. Small Angle X-Ray Scattering, FTIR and SEM Characterization of Nanostructured PVA/TEOS Hybrids by Chemical Crosslinking. *MRS Online Proc. Library* **2005**, *873*, No. K1.9.

(24) dos Reis, E. F.; Campos, F. S.; Lage, A. P.; Leite, R. C.; Heneine, L. G.; Vasconcelos, W. L.; Lobato, Z. I. P.; Mansur, H. S. Synthesis and characterization of poly (vinyl alcohol) hydrogels and hybrids for rMPB70 protein adsorption. *Mater. Res.* **2006**, *9*, 185−191.

(25) Upadhyay, D. J.; Bhat, N. V. Separation of azeotropic mixture using modified PVA membrane. *J. Membr. Sci.* **2005**, *255*, 181−186.

(26) Gillgren, T.; Barker, S. A.; Belton, P. S.; Georget, D. M. R.; Stading, M. Plasticization of zein: A thermomechanical, FTIR, and dielectric study. *Biomacromolecules* **2009**, *10*, 1135−1139.

(27) Distantina, S.; et al. Synthesis of Cross-Linked Konjac Glucomannan and Kappa Carrageenan Film with Glutaraldehyde. *Int. J. Chem. Mol. Eng.* **2015**, *9*, 1014−1017.

(28) Kuchaiyaphum, P.; Yamauchi, T.; Watanesk, R.; Watanesk, S. Hydrophobicity enhancement of the polyvinyl alcohol/rice starch/silk fibroin films by glycerol. *Appl. Mech. Mater.* **2014**, *446−447*, 360−365.